Optimization of tumor immunotherapy in breast carcinoma. Tumor microvasculature normalization: blood vessels' endothelium.

Trabajo Fin de Grado

Grado en Bioquímica

Curso 2020-2021

Autora: Patricia Fierro Hernández

Tutora: Ana Rouzaut Subirá

TABLE OF CONTENTS

SUMMARY.

Breast cancer is one of the most common and malignant cancers nowadays. Like many cancers, it is extensively regulated by pro-angiogenic and pro-lymphangiogenic factors, which induce rapid vasculature growth. This results in aberrant vessels which enhance a pro-tumor environment by preventing treatment against cancer to get to the tumor, inducing the malignancy of cancer cells, and inhibiting the immune response. In the last years, anti-angiogenic treatment was suggested as a possible way to eliminate the tumor-supporting environment. This approach was soon replaced by the judicious use of these anti-angiogenic molecules in normalizing concentrations, to prevent pro-tumor effects, such as cell malignification. In a novel approach to prevent these processes to occur, we have designed a treatment based on the normalization of the tumoral vasculature of triple-negative breast carcinoma, so they return to their physiological state. For this aim, we have analyzed the effects of the blockage of VEGF-A and VEGF-C signaling pathways (angiogenesis and lymphangiogenesis), by targeting their receptors, VEGFR2 and VEGFR3, with inhibitor molecules (DC101 antibody and SAR131675 molecules).

ABBREVIATIONS.

VEGF: vascular endothelial growth factor, VEGFR: vascular endothelial growth factor receptor, TME: tumor microenvironment, Col lV: collagen IV, NG2: neural/glial 2 molecule, VECAD: vascular endothelial cadherin (VE-Cadherin), MFI: mean fluorescence intensity, DC101: antibody against VEGFR2, SAR131675: antibody against VEGFR3.

HYPOTHESIS.

Anti-angiogenesis therapy at low, normalizing concentrations, restructures blood vessels' endothelium and slows down vascular hyperplasia in tumors, improving immune response and anti-tumor therapies' efficiency.

OBJECTIVES.

1- To determine the expression of the pro-angiogenic (VEGF-A) and pro-lymphangiogenic (VEGF-C) molecule in murine breast cancer E0771.

2- To establish a method for the quantification of vascular normalization in samples obtained from E0771 xenografted tumors.

3- To analyze the impact of treatment of mouse carrying E0771 breast tumors with normalizing doses of VEGF-A and VEGF-C signaling inhibitors.

INTRODUCTION.

CANCER.

Cancer is a set of genetic conditions, due to mutations in oncogenes or cancer repressor genes (1). Some cancers may occur due to a sporadic mutation in the genome of some cells and others might be caused by environmental factors (2). Nowadays, cancer is a rising disease due to the population increase (and its lifetime) and the developed-countries lifestyle.

Every neoplastic transformation is characterized by fixed trademarks (3), already described by Douglas Hanahan and Robert Weinberg (4). They are as follows: mutations and genomic instability, high proliferation rate, inhibition of growth suppressing signaling, inhibition of programmed death, unlimited replication rate, angiogenesis induction, metastases, metabolism change, immune system inhibition, and inflammation.

When a tumor appears in the organism, the immune system starts an immune response against the malignant cells that encompass the participation of immune cells, soluble factors, and cytotoxic molecules. Leukocytes or white blood cells are a group of cells derived from bone marrow precursors that are involved in the defense of the organism from internal or external pathogens. At the onset of cancer, leukocytes get to the tumor through the tumor vasculature. Under normal conditions, the endothelium constitutes a barrier that separates leukocytes from tissue stroma. In order to get to the tissue, the active transmigration of leukocytes across the vasculature is tightly regulated by chemokines and surface adhesion molecules such as integrins. At the same time, tissue patrolling leukocytes need to abandon the tissue and present peripheral antigens for tolerance in the adjacent lymph nodes. This inverse migration is mostly performed through the lymphatic vasculature and regulated through parallel but molecularly different mechanisms.

Under inflammatory conditions or in the instance of cancer, leukocyte transit is fueled by the secretion of pro-inflammatory factors from the damaged stroma. In cancer, the primary inflammatory signals induce an increment in blood vessel permeability and an initial influx of naïve leukocytes. Once in the tumor, these cells may engulf tumor antigens and carry them to the lymph nodes to further implement a competent immune response. Nonetheless, the immune response against tumors has to face several challenges. Tumor cells pervade the stability of the vascular niche by producing angiogenic factors that induce their aberrant proliferation. The most prominent angiogenic factor produced by tumor cells is the vascular endothelial growth factor A (VEGF-A) (5). As a result of the action of pro-angiogenic factors, the tumor-associated vasculature is usually unstable, tortuous, and leaky, facilitating tumor cell evasion to distant sites as we will see below.

Breast cancer is one of the most common and malignant cancers in our modern society. It is the most common cancer among women and the second in the general population. Over one million new cases are diagnosed globally per year with a death rate of 33% (6). The malignancy of breast cancer is due to the multiple metastases that are commonly settled principally in the lymphatic nodules. Besides signaling through VEGFA, this type of cancer may involve signaling through vascular endothelial growth factor C (VEGF-C) (7, 8, 9), whose receptor is the vascular endothelial growth factor receptor 3 (VEGFR3). This factor induces lymphangiogenesis, which is the proliferation of new lymphatic vessels that drive immune cells to the lymph nodes. In a cancer situation, the amount of VEGF-C produced

induces an enhanced growth rate, which results in the formation of abnormal, more permeable vessels. This condition has been associated with a worse prognosis in breast cancer patients because of the negative processes induced by this signaling pathway, such as increment of metastases rate or immunosuppression by changes in the infiltration of cancer cells, $TCD4^+$ inflammatory cells, and myeloid suppressor cells (7, 10-12). In addition, VEGF-C facilitates myeloid cell transformation towards pro-tumor phenotype. In sum, VEGF-C signaling induces lymphangiogenesis, that is the formation of abnormal, more permeable lymphatic vessels, which facilitate tumor metastases (6).

TUMOR VASCULATURE.

Blood vessels have essential functions that consist of driving nutrients and oxygen to all the tissues composing the organism. For this aim, they are required to maintain a proper structure that enables elasticity and selective permeability. In their inner side, all of the blood vessels show a layer of endothelial cells, strongly attached by adherent cell-cell junctions. These junctions contain vascular endothelial cadherin (VECAD) which is a calcium-dependent cell adhesion glycoprotein, containing six different extracellular cadherin repeats, a transcellular region, and a short cytoplasmic tail. The endothelial layer is covered in its stroma aspect by the basal membrane, which contains type IV collagen (Col lV). In addition, capillaries and venules present a further layer of pericytes embedded in the connective tissue, that expresses neuron glial molecule antigen (NG2) and an integral membrane chondroitin sulfate proteoglycan that is expressed (between others) by pericytes and contributes to the stabilization of the vasculature by reinforcing its elasticity and the permeability.

The structure of the lymphatic vasculature differs from blood vasculature in some aspects that convey its function. Conversely to blood vessels, lymphatic capillaries need to be more permeable to allow the traffic of lipids and leukocytes and to maintain tissue hydrostatic pressure. For this aim, the lymphatic capillaries lack pericytes and basal membrane, and their junctions are grouped in a "button" structure along the vessels, leaving open gaps to allow cell transit. Under physiological conditions, leukocyte transit across this vasculature is passive and mostly directed through chemotactic cues (13, 14).

This tightly regulated scenario changes when cancer develops within a tissue. Tumors need a high intake of oxygen and nutrients to support their proliferation. To achieve this, most of the solid tumors induce their own vasculature by secreting pro-angiogenic and pro-lymphangiogenic growth factors (5). The development of tumor vasculature is characterized by an extremely high proliferation rate, which leads to an aberrant and inefficient structure of the vessels. As a result, these newly formed vessels are irregular and have an abnormal structure characterized by endothelial loss of polarity and detachment from the vessel wall. Furthermore, tight junctions are commonly incompletely formed, leading to leaky vessels. In this situation, the vascular basement membrane, which acts as a scaffold for endothelium cells and pericytes, turns to be discontinuous and thinner, failing to maintain the vessel structure and increasing its leakiness. Finally, pericytes detach from the endothelium and as a result, the vessel becomes less contractile. Thus, they are unable to regulate blood flow and permeability correctly (10).

Between the angiogenic factors secreted by tumor cells, the family of vascular endothelial growth factor molecules (VEGFs) is of key importance. These proteins are dimeric glycoproteins secreted by many cells, such as fibroblasts, macrophages, platelets,

keratinocytes and mesangial cells, and cancer cells (15, 16). Although there are several members of this family, the most important for cancer progression and metastases are the isoforms VEGF-A and VEGF-C, which induce angiogenesis and lymphangiogenesis respectively.

All endothelial growth factors exert their functions through their binding to dimeric tyrosine kinase-like receptors, the vascular endothelial growth factor receptors. For example, VEGF-A binds to VEGFR2 dimers or VEGFR2/VEGFR3 dimers and VEGF-C binds to VEGFR3 dimers. Activation of these receptors by transphosphorylation leads to signaling towards the cytoplasm and the enhancement of proliferation, cytoskeleton reorganization, and survival pathways in the cells (17). Also, tumor hypoxia induces the production of VEGF-A through the expression and stabilization of the hypoxia-inducible factor 1alpha (HIF-1alpha) that directly binds and activates its promoter (18-20). In this manner, hypoxia further supports the aggressiveness of cancerous cells (by selecting malignant clones) and vessel leakage (by inducing VEGF-A signaling), that induces metastasis and treatment resistance (21).

In this sense, the inhibition of VEGFR2 proteins has been proved to be important in inhibiting angiogenesis and tumor growth, while inhibiting VEGFR3, precludes lymphangiogenesis and metastases in several solid carcinomas (7, 22, 23). In addition, recent studies have shown that the combination treatment with anti-VEGFR2 and anti-VEGFR3 antibodies could potentially decrease lymph node and lung metastases in a more efficient way than inhibiting each protein separately (24).

IMMUNOTHERAPY STRATEGIES.

Nowadays, tumor immunotherapy based on the blockage of immunologic restriction points has become a promising alternative treatment against cancer. This therapy is based on the knowledge that solid tumor cells express concrete molecules, which are involved in the immune response modulation, such as PD-L1 and CTLA-4 membrane proteins, which inhibit T cells' function. Tumors can take advantage of these molecules by using them to escape from the immune response, but this conversion can be blocked by targeting these molecules with blocking antibodies, inhibiting cancer cells' surveillance from the immune response. Immune checkpoints blockade has shown promising results in studies performed in some cancers, such as metastatic melanoma (25, 26), NSCLC (27), bladder cancer (28), Hodgkin lymphoma (29) and ovarian cancer (30), by inhibiting tumor surveillance from the immune response. Even though nobody can argue that this approach constitutes a huge progress for cancer treatment, tumor immunotherapy still needs to be optimized. Only around 20% of the patients suffering from different types of solid tumors, experience a positive effect due to immunotherapy (31-33). This may be in part a consequence of non-proper lymphocyte circulation across the vessels in the tumor microenvironment (TME). Concretely, breast cancer remains a poorly immunogenic tumor, which results in a lower response to immunotherapy. Its objective response rate of PD-1/PD-L1 blockade monotherapy from early-phase trials is only 5.2% to 18.5% (34). In order to improve the recruitment of lymphocytes, normalization of tumor vessel structure by low doses anti-angiogenic therapy may be of benefit. For instance, in a study performed by Huang *et al*., it was demonstrated that treatment with low-dose anti-angiogenic molecule administration increased T lymphocyte infiltration and induced tumor-associated macrophages to polarize toward an immune-stimulatory M1 phenotype (34-37).

Immunotherapy with immune checkpoint inhibitors is not as efficient in breast cancer as it is in other solid tumors like melanoma and lung cancer, since breast cancer is a low immunogenic cancer. Several strategies have been tried out to improve the efficacy of this approach, such as combination with other therapies in order to modify the tumor immune microenvironment. An example of this approach is the concomitant administration of radiotherapy (38), which entails the control of disease and its systemic effects. But again, radiotherapy may in some instances induce immunosuppression (39). Therefore, exploration of new strategies to overcome immunosuppression is of utmost importance in this type of cancer. Some shreds of evidence point to the importance of reducing myeloid suppressor populations which is one of the effects coming from anti-angiogenic therapy (35).

VESSEL NORMALIZATION.

Tumor anti-angiogenic therapies have been used for more than forty years for the treatment of cancer. These were intended to block tumor vessels to starve solid tumors and induce their death (40). Contrary to what was expected, prolonged antiangiogenic treatments were found to be counterproductive. Complete inhibition of tumor vascularization induced increments in tumor hypoxia, which eventually resulted in the selection of more aggressive cancer cells. This condition also affected the tumor immune phenotype: it reprogramed immune cells to a tumor-inducing phenotype, promoting the polarization of the tumor-associated macrophages in the TME to an M2-like phenotype, which suppresses T cell immunity (41, 42), limiting dendritic and T cells' activity and reducing $TCD8^+$ function while increasing $TCD4^+$ regulatory function (43).

In consequence, as an alternative to anti-angiogenic therapies, in 2001, Rakesh Jain proposed the rational use of these molecules at lowered dosage, in a process called normalization of vessels. A normalization treatment aims to fortify TME vessels so that they return to their normal structure, which improves the immune response by leukocyte recruitment, as well as treatment efficiency. The fortification of the vessels includes basal membrane proper structure, cell-cell junction maintenance, and pericyte recruiting coating the vessels. Moreover, normalizing-dose anti-angiogenic treatment, has been demonstrated to polarize tumor-associated macrophages towards tumor aggressive M1-like phenotypes, that increment certain chemokine levels, such as CXCL-9, and CXCL-11, enhancing the recruitment of $TCD8^+$ (35) and helping to establish an immuno-supportive environment.

As previously stated, leukocyte action is key for achieving an efficient immune response against the tumor. Leukocyte proper trafficking depends on well-structured and functional vessels that enable immune cells to get to the tumor. This does not happen in the TME, where vessels have an aberrant structure. A large number of clinical trials are studying new ways to restore the physiological structure of the tumor vessels in order to improve leukocyte recruitment and to enhance treatment outcomes for cancer patients. This implies exploring new treatments, such as combining immunotherapy with vessel normalization treatments.

An example of the use of normalization therapies is the use of sunitinib, an antibody that inhibits VEGFR2 in B16 murine melanoma, which has shown quite an improvement in vessel normalization (44). However, as already said before, this type of therapy shows limited efficiency by itself. The patient's outcome might be improved by combining a normalization treatment and immunotherapy. Moreover, judicious use of anti-angiogenic molecules is complicated due to the heterogeneity of tumors: malignant mutations cause variations in the

angiogenic capacity among different tumors and even within the same tumor mass. Furthermore, other TME components, such as fibroblasts, may contribute to these heterogeneities.

Although the normalization hypothesis was originally proposed to treat solid tumors, it has been used in other diseases which are characterized by abnormal vessels, including tuberculosis (45), neurofibromatosis-2 (NF-2) (46), skin psoriasis, rheumatoid arthritis, and neurodegenerative diseases (10).

Being VEGFR2 and VEGFR3 utterly important signaling pathways involved in breast cancer angiogenesis, the blockage of these receptors might be an interesting approach in breast cancer treatment, improving immune response against the tumor, as well as inhibiting metastases rate to lymphatic ganglia. In this work, we have analyzed the changes in the phenotype of the tumor-associated vasculature, after anti-angiogenic therapy at tumor normalizing dosage in a xenograft model of mouse breast cancer.

EXPERIMENTAL PROCEDURES.

CELLULAR CULTURE.

For in vitro assays several cellular lines were used. These were triple-negative mammal carcinoma cells E0771 (Tebu-Bio, Barcelona, Spain) and murine melanoma B16 expressing ovalbumin antigen B16-F10-OVA (OVA257 epitope) (donated by Dr. Ignacio Melero, CIMA, Pamplona, Spain)

E0771 cells were cultured in T75 and T125 flasks in DMEM medium supplemented with 10% fetal bovine serum (Gibco, Carlsbad, CA, EE.UU.). B16, THP-1, and U937 cells were cultured in T75, T125 flasks with RPMI 1640 medium supplemented with 10% FBS, 100 U/mL penicillin/streptomycin, and $5x10^{-5}$ M 2-mercaptoethanol (Gibco, Carlsbad, CA, EE.UU.). They were cultured in 37ºC, 100% humidity, and 5% CO_2 conditions.

RT-PCR.

1. RNA extraction.

RNA extraction was carried out from -80ºC frozen pellets (for at least 24h) of 1 million cells per pellet or from cultured cells. Firstly, they were centrifugated (Marshall Scientifics centrifuge 5415R) at 1500 rpm for 5 minutes. The pellet was resuspended on 1 mL of TRIzol (Invitrogen, Carlsbad, CA, EE.UU.) and maintained at room temperature for 5 minutes. Then 200 mL of chloroform (Sigma-Aldrich, St. Louis, MO, EE.UU.) were added. After shaking it vigorously, the mixture was maintained at room temperature for another 5 minutes. When the time was passed, samples were centrifugated at 2000 rpm and 4ºC for 15 minutes. Subsequently, 500 µL of isopropanol (Sigma-Aldrich, St. Louis, MO, EE.UU.) were added to the supernatant (500 mL per 1 mL TRIzol). At this point we tended to maintain the samples overnight at -20ºC in isopropanol, so the precipitation was carried out more efficiently. Later, the samples were centrifugated again at 2000 rpm and 4ºC for 10 minutes. Afterward, 500 µL of 70% ethanol were added to the pellet (500 µL per 1 mL TRIzol) and samples were again centrifugated, this time at 8900 rpm and 4ºC for 5 minutes. Finally, the pellet was resuspended in approximately 20 µL nuclease-free H_2O (Invitrogen, Carlsbad, CA, EE.UU.). The quality of the extraction was quantified in a spectrophotometer NanoDrop (ND-1000) by reading samples' absorbance at 260 and 280 nm wavelength.

2. Retrotranscription (RT).

1g of the RNA extracted was retrotranscribed to cDNA using murine myeloma leukemia virus inverse retrotranscriptase (M-MLV RT). A reaction was carried out as follows: 1g cDNA, 2 µL 100 ng/µL hexamers (random primers), 2 µL 10 mM dNTPs, 4 µL M-MLV RT buffer, 1 µL DTT, 1 µL M-MLV RT (everything from Invitrogen, Carlsbad, CA, EE.UU.) volume up to 20 µL of nuclease-free H_2O. The reaction took place for 1 hour at 37ºC in a thermocycler (Marshall Scientific Mastercycler gradient). Finally, samples underwent denaturalization for 10 minutes at 75ºC, to stop the reaction.

3. Polymerase chain reaction (PCR).

Once obtained the cDNA, the expression of several molecules was assessed by polymerase chain reaction (PCR). The molecules that were quantified were beta-actin, VEGF-A, VEGF-C, VEGFR2, and VEGFR3. The PCR mixture contained: 1 µL cDNA, 10 µL PCR mix (PCR master mix 2X, Promega, Madison, WI, EE.UU.), containing Taq DNA polymerase, dNTPs, $MgCl_2$ and reaction buffers, 1 µL forward primer, and 1 µL reverse primer (Table 1) all from Sigma-Aldrich (St. Louis, MO, EE.UU.), and volume up to 20 µL of nuclease-free H_2O. The reaction was carried out in a thermocycler (Marshall Scientific Mastercycler gradient) with a cycle pattern designed as showed in table 2. cDNA obtained from B16-F10-OVA cells was used to compare the expression of the assessed molecules with E0771 cells. THP1 and U937 cDNA was used as VEGFR3 positive controls.

Primer	Sequence 5'-3'		Concentration	Tm (ºC)	Brand
beta-actin	Fw	CCTGGTGCCTAGGGCG	0,5 µM	61,4	Sigma-Aldrich
	Rv	CCTGGTGCCTAGGGCG	0,5 µM	56,8	Sigma-Aldrich
VEFG-A	Fw	GAGTGCCCACTGAGGAGTC	0,5 µM	58	Sigma-Aldrich
	Rv	GCCTCGGCTTGTCACAT	0,5 µM	58	Sigma-Aldrich
VEFG-C	Fw	GTCACCAACATGGAGTCGTG	0,5 µM	58	Sigma-Aldrich
	Rv	CCAGAGATTCCATGCCACTT	0,5 µM	58	Sigma-Aldrich
VEGFR3	Fw	CTGGCAAATGGTTACTCCATGA	0,5 µM	60	Sigma-Aldrich
	Rv	ACAACCCGTGTGTCTTCACTG	0,5 µM	60	Sigma-Aldrich

Table 1. Primers used for PCR reactions. Fw: forward primer, Rv: reverse primer.

STEP	TEMPERATURE (ºC)	TIME	CYCLES
1	95	5'	1
2	94	45"	35
	60	45"	35
	72	1'	35
3	72	7'	1

Table 2. Amplification profile through PCR reaction, used to determine the expression levels of beta-actin, VEGF-A, VEGF-C, VEGFR2, and VEGFR3.

After the PCR reaction, the products obtained were analyzed by electrophoresis in a 1% agarose gel (Agarose D1 low EEO, Pronadisa, Madrid, Spain) in TAE 1X. 20 µL of the samples were loaded with 4 µL of loading buffer 6X (BioLabs, Ipswich, MA, EE.UU.) and 1 µL ethidium bromide (Sigma-Aldrich, St. Louis, MO, EE.UU.). Their molecular weights were estimated comparing to 1 kb ladder molecular weight marker (Gibco, Carlsbad, CA, EE.UU.). 6 µL of the ladder were loaded with 2 µL loading buffer and 1 µL ethidium bromide. The samples underwent an electric field of 90 V during the procedure, for about 1 hour.

ANIMAL MODEL.

Animal handling was performed by authorized personnel (Dr. Alba Yanguas and Dr. Ana Rouzaut) at the animal facility at CIMA (Pamplona, Spain). All the animal procedures have been approved by the animal welfare and ethics committee (Aprob. number 055/18). Here I briefly summarized the experimentation performed to obtain the tissue images that were used in this project.

It was chosen the triple-negative breast carcinoma model (E0771 cancer cells) induced in mice. At the first stage, 500 000 cells/tumor were introduced in each flank of the mouse as shown in figure 1. Eight days later, mice were treated divided into groups with a single dose of an antibody against VEGFR2 (DC101) 10 mg/kg, a combination of DC101 plus a small molecule against VEGFR3 (SAR131675) 50 mg/kg or IgG protein (same concentration as treatment) as a control. Three more doses were provided separated in 3-days intervals (Figure 1). Then, 24 h after the last dose, mice were euthanized and the tumors were extracted. These samples were frozen in OCT (Sakura, Barcelona, Spain) at -80ºC. Then, the tissue was cut in 5-10 µm slices in a cryostat, and samples were finally fixed and stained by immunofluorescence with the corresponding antibodies (table 3). From these tumors, microphotographs were taken with a confocal microscope LSM 800 (Zeiss, Jena, Germany) with an Apochromatic filter 63X (N/A=1.4).

Antibody	Dilution	Reference	Specie	Supplier
CD31	1:50	MEC13.3	Mouse	BD Pharmigen
VE-Cadherin	1:200	ab33168	Rabit	Abacam
VE-Cadherin	1:200	550548	Rat	BD Pharmigen
Collagen IV	1:500	ab19808	Rabit	Abacam
NG2	1:100	ab5320	Rabit	Merck

Table 3. Antibodies used for confocal microscopy.

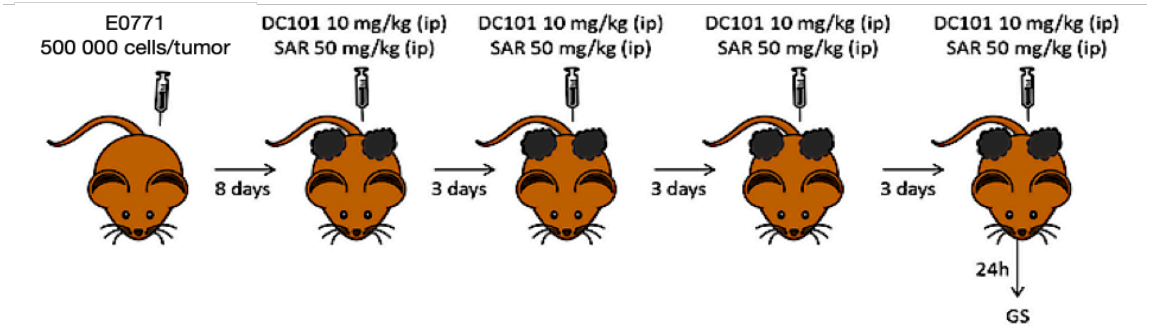

Figure 1. Schematic representation of the animal model used to assess the effect of the four-dose treatment. Scheme of the treatment.

Mice were divided into three different experimental groups as follows: control mice, treated with innocuous IgG (8 mice), single-treatment mice, treated with DC101, an antibody against VEGFR2 (6 mice), and combination-treatment mice, treated with combination therapy of DC101 + SAR131675, a small molecule, an inhibitor of VEGFR3 (6 mice).

IMAGE ANALYSIS.

Vessel normalization rate was quantified by image analysis using ImageJ (FIJI) software. For the analysis of the expression of blood vessels' molecules, the mean fluorescence intensity (MFI) was measured for each molecule (CD31, collagen IV, VE-Cadherin, and NG2). To obtain this, a region of interest (ROI) was determined manually around each vessel in a composite image and was then applied to each channel (each showing the expression of one molecule).

Ten different vessels from each tumor were photographed. A total number of 8 tumors were analyzed in each control group and 6 tumors were analyzed in each treated group.

STATISTICAL ANALYSIS

Statistical analysis was performed by two different programs: SPSS and GraphPad (software Prism 8). Firstly, a normality test was performed in SPSS, concretely a Kolmogorov-Smirnov test, which resulted in an abnormal distribution of the values ($p<0,0001$). Then, the significance was calculated by non-parametric tests such as the U Mann-Whitney test. Three parameters were statistically studied for each channel: total vessel area, labeled vessel area, and mean fluorescence intensity. These were calculated for each group (control, DC101 treatment, and combination treatment) and compared to each other. In every case, the significance was marked as * ($p<0,05$), ** ($p<0,01$), *** ($p< 0,001$) or **** ($p<0,0001$) respectively.

RESULTS.

1- *EXPRESSION OF THE PRO-ANGIOGENIC (VEGF-A) AND PRO-LYMPHANGIOGENIC (VEGF-C) MOLECULE IN THE MOUSE BREAST CANCER E0771.*

First, we wanted to study the expression of the pro-angiogenic (VEGF-A) and pro-lymphangiogenic (VEGF-C) molecules in the mouse breast cancer E0771 cells. For this aim, we performed a PCR with E0771 extracted RNA for VEGF-A and VEGF-C. After the reaction, we obtained that both VEGF-A and VEGF-C molecules were expressed in E0771 but in a low concentration, being VEGF-C expression lower (Figure 2).

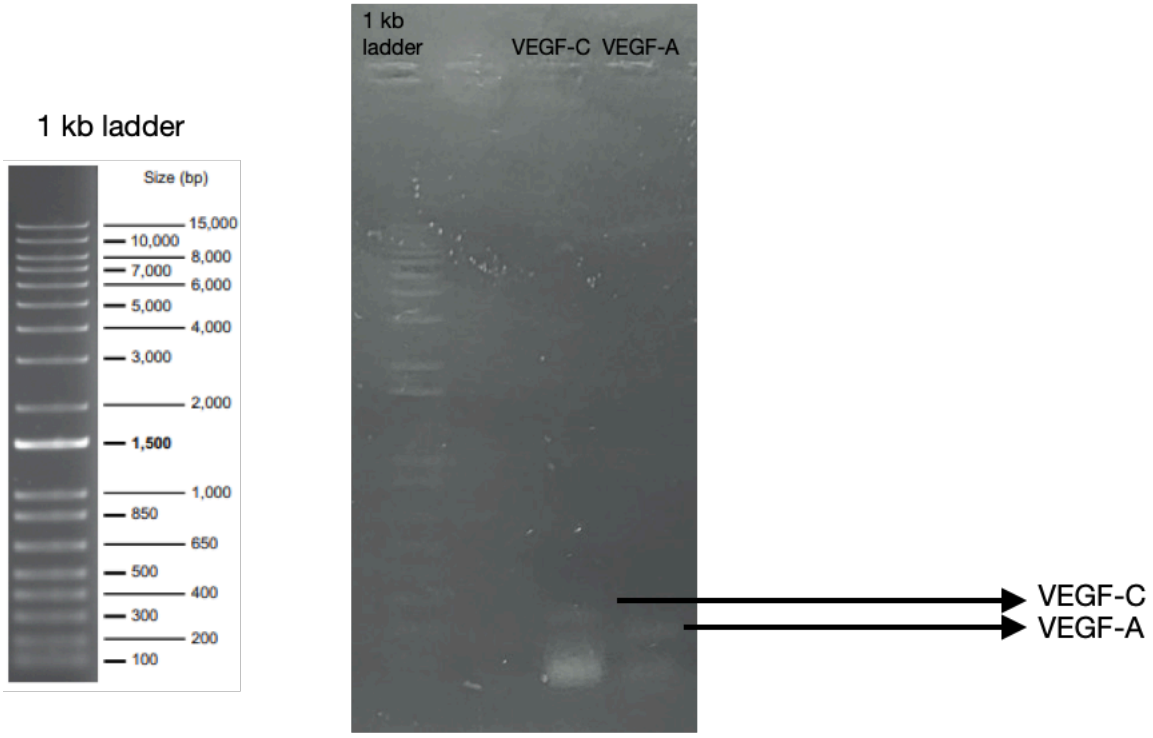

Figure 2. Photograph of the electrophoresis agarose gel with the PCR results from VEGF-C, VEGF-A expression in E0771 cells. The first well represents 1 kB ladder molecular weight marker, the third well shows two bands, VEGF-C (≈ 200 bp) and unbound primers'(below 100 bp), and the fourth well shows two other bands, VEGF-A (≈ 200 bp) and unbound primers' (below 100 bp).

2- ESTABLISHMENT OF A METHOD FOR THE QUANTIFICATION OF VASCULAR NORMALISATION IN SAMPLES OBTAINED FROM E0771 XENOGRAPHTED TUMORS.

2.1- Image acquisition in Zeiss LSM 800 confocal microscope using Zeiss ZEN software.

Each slide was inspected and the region containing one vessel was selected. Images were captured using a confocal microscope LSM800 (Zeiss, Jena, Germany) applying a 63X Apochromatic filter (NA=1.4). 0,2 µm slides were taken that covered the complete vessel depth (stack) by manually setting up the size of the stack for each vessel. The number of images (stacks) per vessel varied depending on the vessel depth and were named sequentially.

Each image was sequentially captured using the filters corresponding to the four wavelengths of emission of the fluorochromes used to label samples: 405, 422, 594, and 647nm.

Previous to the quantification of the expression of each of the molecules, all the stacks corresponding to a vessel were integrated into a single image using Zeiss software in such a manner that each one of these individual images could be analyzed with ImageJ software.

2.2- Image analysis using ImageJ software.

Images were charged in ImageJ software and automatically they rendered four images, corresponding to each one of the channels: channel 0 (647 nm) showed labeling for (Col IV, NG2 or VECAD), channel 1 (594 nm) showed LYVE1 marking, a molecule present in lymphatic endothelium, channel 2 (488 nm) showed CD31 protein, and channel 3 (405 nm) showed DAPI labeling in the nuclei of the cells. For our project, only channels 0 and 2 were relevant, since we wanted to compare the expression of our normalization markers (VECAD, Col lV and NG2) in $CD31^+$ vessels.

For each stack, the maximum intensity fluorescence was selected in each channel and then both channels were merged in a composite (channel 0 colored in magenta and channel 2 colored in green) (Figure 3C). To delimitate the vessel area, a region of interest (ROI) was manually drawn around the vessel in the composite image (Figure 3C). Using this area as a reference, we applied the ROI to channels 0 and 2, and we analyzed the mean fluorescence intensity and area of each one of the parameters analyzed.

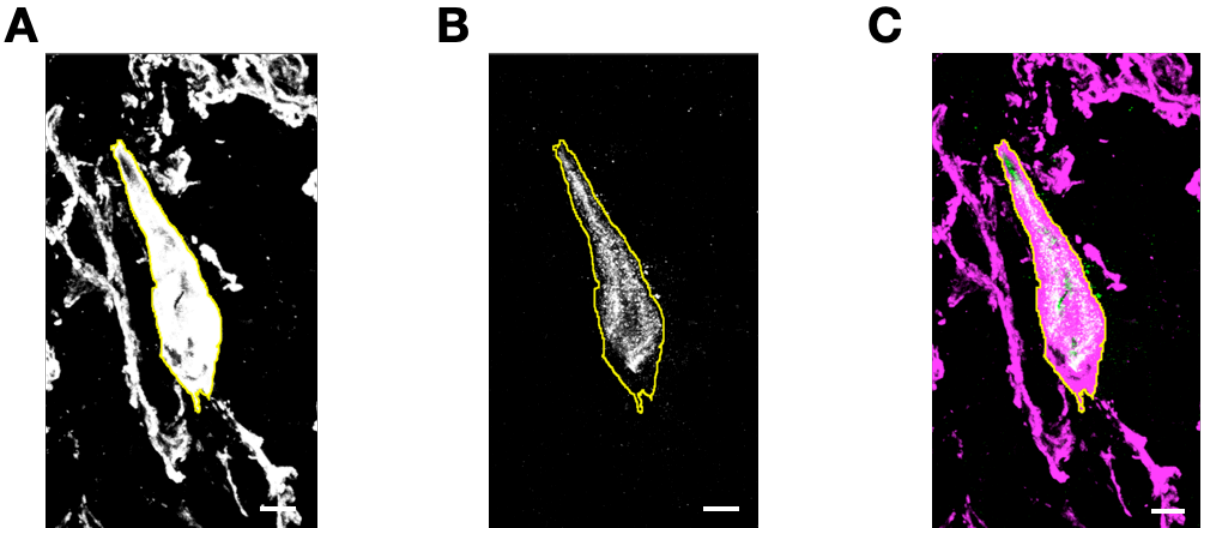

Figure 3. Representative microphotographs of the analysis of the $CD31^+$ blood vessels from E0771tumors, analyzed in ImageJ software. A) Image showing the maximum fluorescence intensity of the labeled protein (collagen IV) in channel 0 (647 nm) and ROI used for the analysis. **(B)** Image showing the maximum fluorescence intensity of CD31 in channel 2 (488 nm) and ROI used for the analysis. **(C)** Composite image after merging channels 0 and 2, where the manually chosen ROI was drawn. 5 µm scale.

3- ANALYSIS OF TREATMENT WITH NORMALISING DOSES OF VEGF-A AND VEGF-C SIGNALING INHIBITORS ON BREAST CANCER TUMOR GROWTH IN A MODEL OF MOUSE CARRYING E0771 BREAST TUMORS.

The core of our work was to analyze whether treatment with low, normalizing doses of anti-angiogenic (DC101, 10 mg/Kg) alone or in combination with anti-lymphangiogenic (SAR131675 50 mg/Kg) molecules was capable of inducing the stabilization of the tumor vasculature. For this aim, we used a model of triple-negative breast carcinoma (E0771 cells) induced in C57BL/6 mice. Tumor vessels from extracted tumors were detected by labeling with anti-CD31/PECAM antibodies. This molecule belongs to the immunoglobulin family of surface receptors and is involved in leukocyte adhesion to endothelial cells and the elimination of aged neutrophils. To describe the changes in the vascular phenotype, antibodies against molecules expressed by endothelial cells, such as collagen IV, NG2, and VE-Cadherin, were used. Microphotographs were taken with a confocal microscope of several vessels per mouse. Images were processed as described above and vessel area (ROI area), mean fluorescence intensity (MFI), and the percentage of total area positive for each marker were calculated. Fluorescence intensity per area was obtained by dividing each vessel's mean fluorescence intensity by its corresponding total area. Then, to compare the results of the treated groups in respect to the controls, we calculated the mean of MFI/area of the controls (IgG treated animals) and we divided each MFI per area from both controls (IgG) and treated groups by this mean value. Statistical differences between groups were analyzed, first by interrogating for normality through the Kolmogorov-Smirnov test. We obtained a non-parametric sample distribution. In consequence, we compared the group's medians by the U Mann-Whitney test.
In the first place, we analyzed whether treatments induced any changes in the overall vessel area (Figure 4). To calculate the vessel area, we used the ROI drawn on the overlay of the fluorochromes, obtained from the two merged channels (channel 0 and 2). When analyzing changes in the area of the treated and non-treated vessels, we found that DC101 antibody significantly diminishes the area compared to non-treated vessels, while combination treatment tends to maintain the size of the vessels (Figure 4).

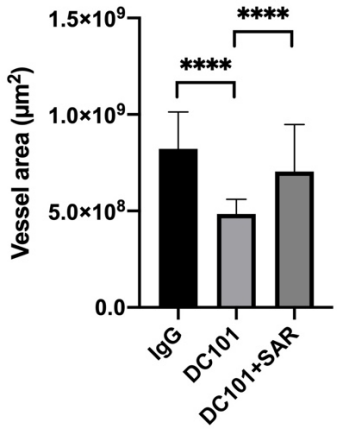

Figure 4. Histogram representing mean area of blood vessels of the E0771 tumors after mice were treated with DC101 and DC101+SAR or IgG as described in Material and Methods. The graphics represent Median at 95% CI (*p<0,05, **p<0,01, ***p<0,001, ****p<0,0001).

Once differences in vessel area were analyzed, we continued analyzing the mean fluorescence per area for each one of the three molecules analyzed.

To inspect for the presence of intercellular adhesion, we compared VE-Cadherin expression between samples. As it is shown in figure 5A, we did not observe any significant difference in VE-Cadherin expression when mice were treated with anti-VEGFR2 antibodies (DC101) and, contrarily to what we expected, combined treatment with DC101 and the VEGFR3 signaling inhibitor, SAR131675, even diminished the intensity of this surface molecule. When we compare the vessel's area occupied by this protein, we find that both treatments significantly reduced the vessel area occupied by this protein, being more drastic in the case of combined treatment (Figure 5B). From these results, we cannot infer any contribution of these treatments to increment the amount of inter-endothelial adhesive junctions.

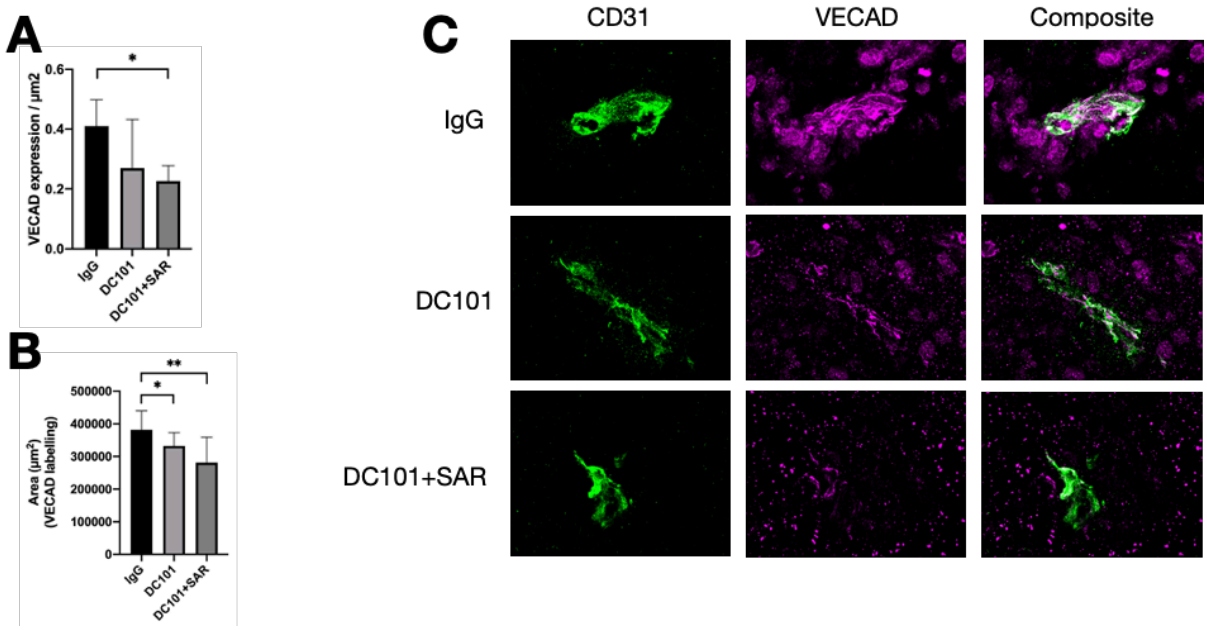

Figure 5. Representation of detection and quantification of VE-Cadherin expression in blood vessels of E0771 tumors after treatment with DC101, DC101+SAR or IgG control, as described in Materials and Methods. (A) Histogram representing median of VECAD fluorescence intensity per square micron in blood vessels of E0771 tumors, after treatment with DC101, DC101+SAR or IgG. **(B)** Histogram representing vessel area occupied by VE-Cadherin after treatment with DC101 and after treatment with DC101+SAR compared to control (IgG). The graphics represent Median at 95% CI (*p<0,05, **p<0,01, ***p<0,001, ****p<0,0001). **(C)** Representative microphotographs of VECAD staining of CD31 positive blood vessels. CD31 (green), VECAD (magenta). Ten vessels were analyzed per tumor and at least 6 mice were analyzed per group. 0,5 µm scale.

The study of the distribution of the basal membrane protein collagen IV rendered different results. DC101 treatment did not induce any significant change in the fluorescence intensity signal per squared area but combined treatment with DC101 and SAR131675 incremented the intensity of its expression in tumor-associated vasculature (Figure 6A). When analyzing the vascular area occupied by this protein, we observed that, as occurred in the case of VE-Cadherin, treatment with DC101 at low dosage diminished the presence of this protein in the tumor-associated vasculature. In contrast, combined treatment with DC101 and SAR131675 lead to collagen IV intensities comparable to those from non-treated samples. (Figure 6B). These results show that although monotherapy with DC101 does not contribute to basal membrane deposition, combined treatment increments its deposition and may contribute to its stabilization.

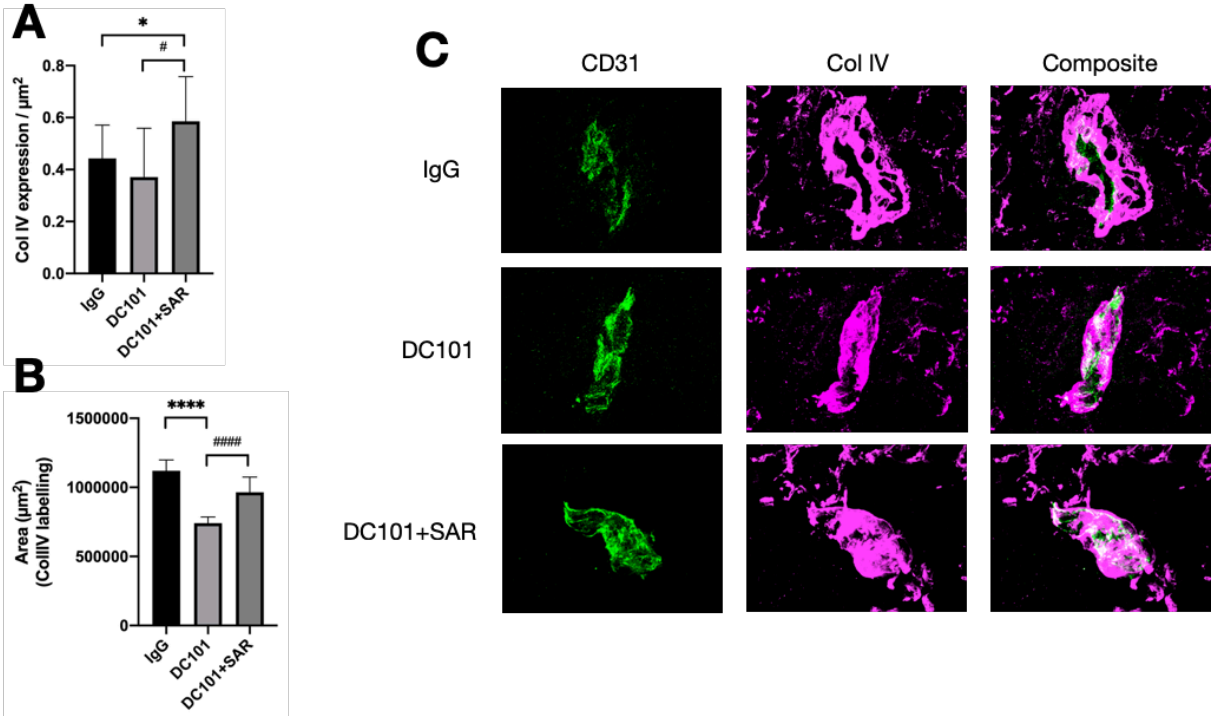

Figure 6. Representation of detection and quantification of collagen IV expression in blood vessels of E0771 tumors after treatment with DC101, DC101+SAR or IgG control, as described in Materials and Methods. (A) Histogram representing median of Col lV fluorescence intensity per square micron in blood vessels of E0771 tumors, after treatment with DC101, DC101+SAR or IgG. **(B)** Histogram representing vessel area occupied by Col lV after treatment with DC101 and after treatment with DC101+SAR compared to control (IgG). The graphics represent Median at 95% CI (*p<0,05, **p<0,01, ***p<0,001, ****p<0,0001). **(C)** Representative microphotographs of Col lV staining of CD31 positive blood vessels. CD31 (green), Col lV (magenta). Ten vessels were analyzed per tumor and at least 6 mice were analyzed per group. 0,5 µm scale.

Finally, we analyzed NG2 expression in the same vessels. We could not find any significant differences in NG2 signal expression between treatments when mice were treated with DC101 alone or in combination with SAR131675 (Figure 7A). Again, when analyzing the vessel area covered by pericytes, significant differences were only found in the combination treatment group (Figure 7B), where the area occupied by NG2 was increased.

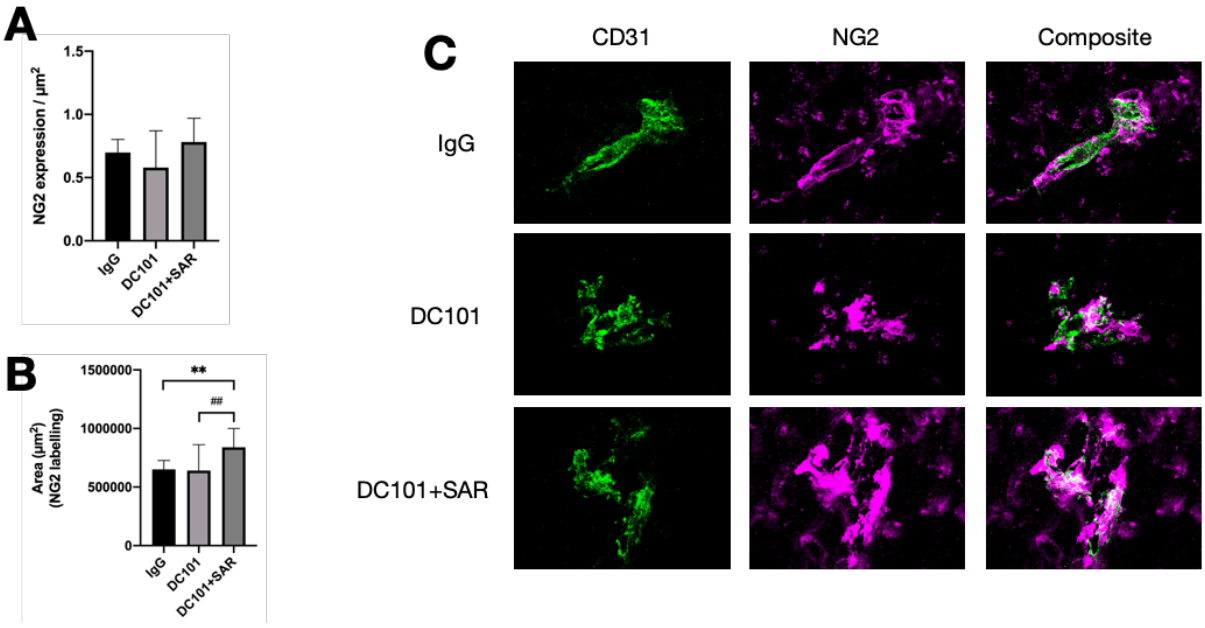

Figure 7. Representation of detection and quantification of NG2 expression in blood vessels of E0771 tumors after treatment with DC101, DC101+SAR or IgG control, as described in Materials and Methods. (A) Histogram representing median of NG2 fluorescence intensity per square micron in blood vessels of E0771 tumors, after treatment with DC101, DC101+SAR or IgG. **(B)** Histogram representing vessel area occupied by NG2 after treatment with DC101 and after treatment with DC101+SAR compared to control (IgG). The graphics represent Median at 95% CI (*p<0,05, **p<0,01, ***p<0,001, ****p<0,0001). **(C)** Representative microphotographs of NG2 staining of CD31 positive blood vessels. CD31 (green), NG2 (magenta). Ten vessels were analyzed per tumor and at least 6 mice were analyzed per group. 0,5 µm scale.

From these results, we deduce that repetitive treatment with the VEGFR2 blocking antibody DC101 at low doses does not contribute to tumor vessel stabilization, while combined treatment with VEGFR3 inhibitor molecules, SAR131675, may contribute to improving vessel condition through incremented stabilization of basal membrane and pericyte coverage, but in a non-significant manner.

DISCUSSION.

Blood vessels present in the TME are chaotic and their structure is aberrant, due to the immense amount of pro-angiogenic factors that are released by tumor cells (5). In fact, the tumor aberrant and leaky vasculature helps metastases, obstructs anti-tumor therapy efficiency, and hampers anti-tumor immune response (10).

The effects of the blockage of tumor vasculature as a therapeutic tool in cancer have been actively studied in the last years. Anti-angiogenic treatment was soon suggested as a possible way to eliminate tumor support, combat metastases, and induce tumor apoptosis. However, despite offering benefits in some instances, such as ovarian cancer, bladder cancer, and tuberculosis (10, 35, 45- 47), monotherapy with anti-angiogenic molecules when maintained for a long time is not successful, since it may cause excessive pruning of the vessels, blocking the infiltration of anti-tumor immune-response cells and resulting in the selection of more aggressive clones (41-43).

Given these inconveniences, some studies have suggested the possibility of using anti-angiogenic molecules with the goal of restoring the physiological phenotype of the endothelial layer and name this strategy as normalization therapy. In this case, in order to achieve a successful outcome (48), it is important to avoid excessive pruning of immature vessels that might lead to hypoxia (18-20). As a result, the administration of lower doses of anti-angiogenic molecules will turn immature vessels to a physiological state, which will improve responses to the treatment against cancer. This normalization treatment uses lower doses of anti-angiogenic molecules, such as anti-VEGF molecules. Between one-eighth and one-half of the anti-angiogenic dose (35, 49).

Normalization treatments with anti-angiogenic molecules are promising novel therapies that have been used as monotherapies and have also been used in combination with immunotherapies. For instance, in a mouse model of breast cancer, it was demonstrated that treatment with a low dose of anti-VEGFR2, sensitized tumor cells to PD-L1 blockade in a dose-dependent way. This resulted in an improvement in the efficacy of the immunotherapy, and the infiltration and efficacy of anti-tumor immune cells (35, 34).

In this project, we wanted to analyze whether it is possible to normalize the tumor blood vasculature in a murine breast carcinoma model. We used a murine triple-negative breast carcinoma (E0771 carcinoma cells), since it has the same features as an aggressive breast cancer in humans, it shows mutations for estrogen, progesterone, and EGFR receptors (50).

First, we detected by non-quantitative PCR the expression of VEGF-A and VEGF-C in E0771 cells. The reaction showed that they both express very low levels of VEGF-A and VEGF-C, being the expression of the last molecule even lower. With these results, we can consider that our tumor model is not very angiogenic, neither lymphangiogenic. In fact, when we have compared the presence of tumor-associated vasculature between xenografts of E0771 tumors and B16 (murine melanoma) tumors, it was significantly lower in the E0771 carcinoma model (data not shown). In fact, it has been seen that depending on the mouse strain used, tumor angiogenesis might vary (57-60). Comparing our C57BL/6 strain to Balb/c strain, it has been demonstrated that Balb/c develops faster a less dense microvasculature net (61), achieving its VEGF-A maximum expression four days before C57BL/6 mice do. We also searched by PCR for the expression of VEGFR3, but we could not detect any expression of this protein in our

tumor model by PCR. This means that the effects of SAR treatment impact the tumor stroma and not directly on the tumor cells.

As normalization treatments, we wanted to assess the normalization effect of the blockage of VEGFR2 and VEGFR3, with inhibitory agents used at low doses. Both VEGFRs form dimers and are present in blood vessels. Angiogenic signaling through VEGFRs occurs mostly through VEGFR2, but tumor vessels aberrantly express VEGFR3. This last receptor is of utmost importance for the survival and maturation of the lymphatic vasculature. In fact, VEGFR3 is involved in metastases, lymphangiogenesis, and also angiogenesis. Therefore targeting this receptor, may constitute an interesting approach in cancer treatment.

Tumors were treated with DC101 antibody and SAR131675 blocking molecules. We based our selection of these agents on previous results of studies where DC101 was used to treat glioblastoma tumors (51) and squamous cell carcinoma (52). The small inhibitory molecule SAR131675 used in mouse models of mammary carcinoma, is a highly selective molecule against VEGFR3 that showed anti-lymphangiogenic activity in vivo by significantly reducing lymphatic node invasion and lung metastases (53, 54).

Regarding the therapeutic doses, we based our calculations of what we called “normalizing” doses, on the results obtained by Rakesh Jain et al., who observed a recovery of the physiological functions and the structure of the tumor vessels, characterized by a normal distribution of endothelial adhesion molecules (49) and an improvement in the responses to PD-L1 immunotherapy when administered at single-dose DC101 of 10 mg/kg (55).

To analyze the efficacy of our treatments we analyzed vessel area in each sample, and the expression of VE-Cadherin (as a proxy of intercellular adhesion), collagen IV (present in the basal membrane), and NG2 (indicative of pericytes coverage).

In the first place, we observed that DC101 treatment significantly reduced vessel area, indicating a diminution in the extent of tumor angiogenesis. Surprisingly, a combination with VEGFR3 inhibitor SAR 131675, lead to a restoration of the vascular area to the same levels as untreated tumors. These results lead us to speculate that, in terms of vascular proliferation, VEGFR3 inhibition promoted somehow signaling through VEGFR2. In fact, there are instances in the bibliography where it is described that the inhibition of VEGFR3 can upregulate VEGFR2-derivated signals. For example, Heinoilanen *et al*. observed that VEGFR3 gene deletion led to increased activity of the VEGFR2 pathway (63). As a result of SAR131675 inhibition against VEGFR3, VEGFR2 would not be sufficiently inhibited by DC101, being the determined dose lower than it would be needed.

When we analyzed by confocal microscopy and posterior image analysis the expression of our normalization markers, we observed that our normalization treatment was counter-effective in terms of the expression of adhesion molecules: both treatments led to diminutions in the area positive (extension of positivity) for VE-Cadherin expression and combinational treatment also significantly diminished the intensity of the signal (number of molecules) per surface unit.

It is known that the VEGFR2 signaling pathway leads to the internalization of VE-Cadherin molecules, resulting in the disruption of endothelial adhesion junctions (62). Thus, blockage of VEGFR2 should restore VE-Cadherin expression levels, restructuring adhesion and preventing leakage. In our study, we have seen that, after the use of DC101 as monotherapy

and in combination with SAR, instead of normalizing the vessels, VEGFR2 blockage actually induces a decrease in the expression of VE-Cadherin. These results indicate that, contrary to what was expected, the adhesion junctions were being disrupted, leading to an enhanced instability of the vessels. This effect has been previously described, since endothelial cells are able to adapt to VEGFR2 blockage, by activating other pro-angiogenic pathways (17), such as FGF or angiopoietin pathways (56). But this matter should be analyzed separately since it is beyond the scope of this study.

The analysis of collagen IV only partially followed this tendency. We observed that DC101 treatment again induced a significant diminution in the area positive for collagen lV and non-significant variations in its intensity when compared against control mice. These results reflect that again, the only possible effect leads to basal membrane destabilization. In contrast, combined treatment with inhibition of VEGFR3 signaling leads to restoration of the area occupied by collagen IV and an increment in the intensity of the signal. We obtain a similar pattern when analyzing pericyte coverage: only the combination of DC101 and SAR131675 induced significant increments in NG2 expression.

In this case, it seemed that treatment with SAR131675 may lead to some vessel stabilization. In this regard, it is important to note that other cells in the stroma may be responsible for VEGFR3 inhibition and induce higher collagen deposition. For example, it has been seen that anti-VEGFR3 therapy results in a switch of tumor-infiltrating myeloid cells from pro-tumor to anti-tumor cells. Tumor-infiltrating macrophages are high VEGF producers being more active than those with suppressor function. The inhibition of this type of macrophages may lead to less VEGF-A in the tumor stroma and contribute to vessel normalization.

To sum up, from our results we may conclude that, despite some stabilization of tumor vasculature, the inhibition of VEGFR2 and VEGFR3 at the dose of anti-angiogenic molecules assayed does not make a significant normalizing effect in tumor vasculature of the E0771 cancer model.

In view of these results, we assume that the main limitation may emanate from the interaction between both receptors, and the dose used. We consider that the dose that we calculated as “normalizing” was not enough to make an effect blocking VEGFR2 in our cancer cells. Therefore, we consider that our experimental models would have been more efficient by raising DC101 concentration while treating mice with DC101 as monotherapy and not in combination with SAR131675. However, DC101 concentration adjustment should be calculated with caution, avoiding reaching beyond-normalizing concentrations, in order to prevent an excessive pruning of the vessels and, therefore, malignancy inducement.

Additionally, it has been described that pharmacologically-induced normalization is characterized by a “normalization window”. This is described as the period after the first dose administration in the treatment. Within the normalization window, the tumor vessels show normalization features. If the therapy is interrupted or if it is maintained for a long time, this window “closes” and the vessels lose their normalization phenotype. We think that the limitations in our study can also be related to this normalization window. We administrated four doses of the inhibitor molecules separated in three-day intervals. Nevertheless, the normalization window in our treatment scheme may start later than we expected initially.

In order to attempt a better approach to vasculature normalization, a dose-response curve should be characterized for each of the treatments, and the normalization window should be described regarding dose administration.

Moreover, cancer cells often do not express VEGFR3 and therefore do not answer to its inhibition Nevertheless, VEGFR3 blockage might impact other tumor stroma cells VEGFR3 positive, such as myeloid tumor-suppressor cells, macrophages, and monocytes (54, 64). In this light, we consider that the normalizing effect that the combination treatment showed in this study regarding collagen IV expression, is due to the inhibition of VEGFR3 located in the tumor stroma.

Finally, concerning the quantification of the vascular normalization by image analysis in ImageJ software, we suggest establishing a computer-based artificial-intelligence program, to determine the ROIs around the vessels avoiding the accumulative effect of a possible systematic error caused by differing criteria.

CONCLUSIONS.

1-Triple-negative breast carcinoma cells express low amounts of VEGF-A and VEGF-C, being the second factor even less expressed and, thus, they are not highly angiogenic and neither lymphangiogenic tumors.

2-Manual analysis of regions of interest is time-consuming and may result in heterogeneity due to subjective appreciation. Thus, it would be advisable to develop an automatic quantification program of these structures.

3- Inhibition of VEGF-A and VEGF-C pro-angiogenic factors by normalizing doses of DC101 antibody and SAR131675 molecule, does not induce the normalization of tumor blood vasculature as read by VECAD, Col IV, and NG2 expression. Normalization of the tumor blood vessels is a heterogeneous process, which might be regulated by many factors, such as tumor stroma cells.

ANNEX I. EVOLUTION OF TUMOR DIAMETER IN MOUSE TREATED WITH ANTI-ANGIOGENIC AND ANTI-LYMPHANGIOGENIC MOLECULES AT NORMALIZING DOSES.

Tumor diameter was measured in three-day intervals after E0771 cells were injected within the mouse, until they were extracted. These results were obtained by Dr. Alba Yanguas for her doctoral thesis, but they are explained below as they supported the results showed in this project.

Tumor diameter from mice treated with DC101 and DC101+SAR were compared to tumor diameter from the control group (Figure 8). The results show a decrease in the tumor diameter from mice treated with DC101 compared to control. Nevertheless, tumor diameter from mice treated with DC101+SAR compared to IgG showed no significant differences.

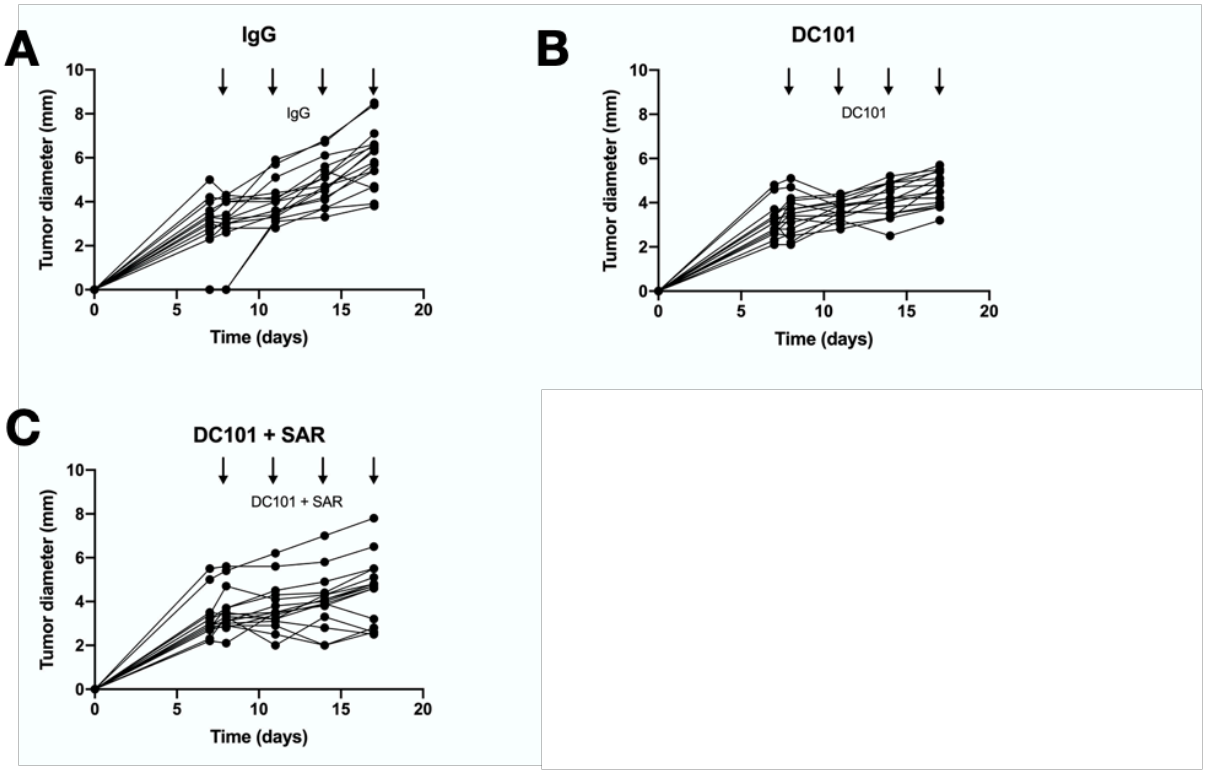

Figure 8. Graphics representing tumor diameter in mice after treatment with DC101, DC101+SAR and IgG, as described in Materials and Methods, in mm. (A) Tumor diameter from control mice. **(B)** Tumor diameter from DC101 treated mice. **(C)** Tumor diameter from DC101+SAR treated mice. The graphics show Mean + SEM.

BIBLIOGRAPHY.

1. Wang L-H, Wu C-F, Rajasekaran N, Shin YK. Loss of tumor suppressor gene function in human cancer: An overview. Cell Physiol Biochem. 2018;51(6):2647–93.

2. Wang Q. Cancer predisposition genes: molecular mechanisms and clinical impact on personalized cancer care: examples of Lynch and HBOC syndromes. Acta Pharmacol Sin. 2016;37(2):143–9.

3. Dai X, Xiang L, Li T, Bai Z. Cancer hallmarks, biomarkers and breast cancer molecular subtypes. J Cancer. 2016;7(10):1281–94.

4. Hanahan D, Weinberg RA. The Hallmarks of Cancer'. Cell. 2000;100(1):57–70.

5. Tan LY, Martini C, Fridlender ZG, Bonder CS, Brown MP, Ebert LM. Control of immune cell entry through the tumour vasculature: a missing link in optimising melanoma immunotherapy? Clin Transl Immunology. 2017;6(3):e134.

6. Hashemi V, Maleki LA, Esmaily M, Masjedi A, Ghalamfarsa G, Namdar A, et al. Regulatory T cells in breast cancer as a potent anti-cancer therapeutic target. Int Immunopharmacol. 2020;78(106087):106087.

7. Skobe M, Hawighorst T, Jackson DG, Prevo R, Janes L, Velasco P, et al. Induction of tumor lymphangiogenesis by VEGF-C promotes breast cancer metastasis. Nat Med. 2001;7(2):192–8.

8. Chen Y, Keskin D, Sugimoto H, Kanasaki K, Phillips PE, Bizarro L, et al. Podoplanin+ tumor lymphatics are rate limiting for breast cancer metastasis. PLoS Biol. 2018;16(12):e2005907.

9. Schoppmann SF, Birner P, Stöckl J, Kalt R, Ullrich R, Caucig C, et al. Tumor-associated macrophages express lymphatic endothelial growth factors and are related to peritumoral lymphangiogenesis. Am J Pathol. 2002;161(3):947–56.

10. Goel S, Duda DG, Xu L, Munn LL, Boucher Y, Fukumura D, et al. Normalization of the vasculature for treatment of cancer and other diseases. Physiol Rev. 2011;91(3):1071–121.

11. Lund AW, Wagner M, Fankhauser M, Steinskog ES, Broggi MA, Spranger S, et al. Lymphatic vessels regulate immune microenvironments in human and murine melanoma. J Clin Invest. 2016;126(9):3389–402.

12. Kataru RP, Ly CL, Shin J, Park HJ, Baik JE, Rehal S, et al. Tumor lymphatic function regulates tumor inflammatory and immunosuppressive microenvironments. Cancer Immunol Res. 2019;7(8):1345–58.

13. Yanguas A, Garasa S, Teijeira Á, Aubá C, Melero I, Rouzaut A. ICAM-1-LFA-1 dependent CD8+ T-lymphocyte aggregation in tumor tissue prevents recirculation to draining lymph nodes. Front Immunol. 2018;9:2084.

14. Teijeira A, Hunter MC, Russo E, Proulx ST, Frei T, Debes GF, et al. T cell migration from inflamed skin to draining lymph nodes requires intralymphatic crawling supported by ICAM-1/LFA-1 interactions. Cell Rep. 2017;18(4):857–65.

15. Bvsalud.org. [citado el 15 de abril de 2021]. Disponible en: https://docs.bvsalud.org/biblioref/2018/09/877818/1255-texto-del-articulo-5667-1-10-20171022.pdf

16. Lu Y, Qin T, Li J, Wang L, Zhang Q, Jiang Z, et al. MicroRNA-140-5p inhibits invasion and angiogenesis through targeting VEGF-A in breast cancer. Cancer Gene Ther. 2017;24(9):386–92.

17. Shibuya M. Differential roles of vascular endothelial growth factor receptor-1 and receptor-2 in angiogenesis. BMB Rep. 2006;39(5):469–78.

18. Fukumura D, Kloepper J, Amoozgar Z, Duda DG, Jain RK. Enhancing cancer immunotherapy using antiangiogenics: opportunities and challenges. Nat Rev Clin Oncol. 2018;15(5):325–40.

19. Hsu M-C, Pan M-R, Hung W-C. Two birds, one stone: Double hits on tumor growth and lymphangiogenesis by targeting vascular endothelial growth factor receptor 3. Cells. 2019;8(3):270.

20. Li X, Gao Y, Li J, Zhang K, Han J, Li W, et al. FOXP3 inhibits angiogenesis by downregulating VEGF in breast cancer. Cell Death Dis [Internet]. 2018;9(7). Disponible en: http://dx.doi.org/10.1038/s41419-018-0790-8

21. Martin JD, Seano G, Jain RK. Normalizing function of tumor vessels: Progress, opportunities, and challenges. Annu Rev Physiol. 2019;81(1):505–34.

22. Harris AR, Perez MJ, Munson JM. Docetaxel facilitates lymphatic-tumor crosstalk to promote lymphangiogenesis and cancer progression. BMC Cancer [Internet]. 2018;18(1). Disponible en: http://dx.doi.org/10.1186/s12885-018-4619-8

23. Dufies M, Giuliano S, Ambrosetti D, Claren A, Ndiaye PD, Mastri M, et al. Sunitinib stimulates expression of VEGFC by tumor cells and promotes lymphangiogenesis in clear cell renal cell carcinomas. Cancer Res. 2017;77(5):1212–26.

24. Roberts N, Kloos B, Cassella M, Podgrabinska S, Persaud K, Wu Y, et al. Inhibition of VEGFR-3 activation with the antagonistic antibody more potently suppresses lymph node and distant metastases than inactivation of VEGFR-2. Cancer Res. 2006;fg(5):2650–7.

25. Hodi FS, O'Day SJ, McDermott DF, Weber RW, Sosman JA, Haanen JB, et al. Improved survival with ipilimumab in patients with metastatic melanoma. N Engl J Med. 2010;363(8):711–23.

26. Robert C, Thomas L, Bondarenko I, O'Day S, Weber J, Garbe C, et al. Ipilimumab plus dacarbazine for previously untreated metastatic melanoma. N Engl J Med. 2011;364(26):2517–26.

27. Motzer RJ, Escudier B, McDermott DF, George S, Hammers HJ, Srinivas S, et al. Nivolumab versus everolimus in advanced renal-cell carcinoma. N Engl J Med. 2015;373(19):1803–13.

28. Powles T, Eder JP, Fine GD, Braiteh FS, Loriot Y, Cruz C, et al. MPDL3280A (anti-PD-L1) treatment leads to clinical activity in metastatic bladder cancer. Nature. 2014;515(7528):558–62.

29. Ansell SM, Lesokhin AM, Borrello I, Halwani A, Scott EC, Gutierrez M, et al. PD-1 blockade with nivolumab in relapsed or refractory Hodgkin's lymphoma. N Engl J Med. 2015;372(4):311–9.

30. Hamanishi J, Mandai M, Ikeda T, Minami M, Kawaguchi A, Murayama T, et al. Safety and antitumor activity of anti-PD-1 antibody, nivolumab, in patients with platinum-resistant ovarian cancer. J Clin Oncol. 2015;33(34):4015–22.

31. Sugie T. Immunotherapy for metastatic breast cancer. Chin Clin Oncol. 2018;7(3):28.

32. Koppolu V, Rekha Vasigala V. Checkpoint immunotherapy by nivolumab for treatment of metastatic melanoma. J Cancer Res Ther. 2018;0(0):0.

33. Rodríguez-Cerdeira C, Carnero Gregorio M, López-Barcenas A, Sánchez-Blanco E, Sánchez-Blanco B, Fabbrocini G, et al. Advances in immunotherapy for melanoma: A comprehensive review. Mediators Inflamm. 2017;2017:1–14.

34. Li Q, Wang Y, Jia W, Deng H, Li G, Deng W, et al. Low-dose anti-angiogenic therapy sensitizes breast cancer to PD-1 blockade. Clin Cancer Res. 2020;26(7):1712–24

35. Huang Y, Yuan J, Righi E, Kamoun WS, Ancukiewicz M, Nezivar J, et al. Vascular normalizing doses of antiangiogenic treatment reprogram the immunosuppressive tumor microenvironment and enhance immunotherapy. Proc Natl Acad Sci U S A. 2012;109(43):17561–6.

36. Jain RK. Antiangiogenesis strategies revisited: From starving tumors to alleviating hypoxia. Cancer Cell. 2014;26(5):605–22.

37. Willett CG, Boucher Y, Duda DG, di Tomaso E, Munn LL, Tong RT, et al. Surrogate markers for antiangiogenic therapy and dose-limiting toxicities for bevacizumab with radiation and chemotherapy: continued experience of a phase I trial in rectal cancer patients. J Clin Oncol. 2005;23(31):8136–9.

38. Teijeira A, Garasa S, Peláez R, Azpilikueta A, Ochoa C, Marré D, et al. Lymphatic endothelium forms integrin-engaging 3D structures during DC transit across inflamed lymphatic vessels. J Invest Dermatol. 2013;133(9):2276–85.

39. Ma L, Gonzalez-Junca A, Zheng Y, Ouyang H, Illa-Bochaca I, Horst KC, et al. Inflammation mediates the development of aggressive breast cancer following radiotherapy. Clin Cancer Res. 2021;27(6):1778–91.

40. Helfrich I, Schadendorf D. Blood vessel maturation, vascular phenotype and angiogenic potential in malignant melanoma: one step forward for overcoming anti-angiogenic drug resistance? Mol Oncol. 2011;5(2):137–49.

41. Palazon A, Tyrakis PA, Macias D, Veliça P, Rundqvist H, Fitzpatrick S, et al. An HIF-1α/VEGF-A Axis in Cytotoxic T Cells Regulates Tumor Progression. Cancer Cell. 2017;32(5):669-683.e5.

42. Engblom C, Pfirschke C, Pittet MJ. The role of myeloid cells in cancer therapies. Nat Rev Cancer. 2016;16(7):447–62.

43. Clever D, Roychoudhuri R, Constantinides MG, Askenase MH, Sukumar M, Klebanoff CA, et al. Oxygen sensing by T cells establishes an immunologically tolerant metastatic niche. Cell. 2016;166(5):1117-1131.e14.

44. Huang H, Langenkamp E, Georganaki M, Loskog A, Fuchs PF, Dieterich LC, et al. VEGF suppresses T-lymphocyte infiltration in the tumor microenvironment through inhibition of NF-κB-induced endothelial activation. FASEB J. 2015;29(1):227–38.

45. Datta M, Via LE, Kamoun WS, Liu C, Chen W, Seano G, et al. Anti-vascular endothelial growth factor treatment normalizes tuberculosis granuloma vasculature and improves small molecule delivery. Proc Natl Acad Sci U S A. 2015;112(6):1827–32.

46. Plotkin SR, Stemmer-Rachamimov AO, Barker FG 2nd, Halpin C, Padera TP, Tyrrell A, et al. Hearing improvement after bevacizumab in patients with neurofibromatosis type 2. N Engl J Med. 2009;361(4):358–67.

47. Jain RK. Normalizing tumor vasculature with anti-angiogenic therapy : A new paradigm for combination therapy'. Nature Medicine. 2001;8:987–989.

48. Xu L, Fukumura D, Jain RK. Acidic extracellular pH induces vascular endothelial growth factor (VEGF) in human glioblastoma cells via ERK1/2 MAPK signaling pathway: mechanism of low pH-induced VEGF. J Biol Chem. 2002 Mar 29;277(13):11368-74. doi: 10.1074/jbc.M108347200. Epub 2001 Dec 11. Erratum in: J Biol Chem 2002 May 24;277(21):19242. PMID: 11741977.

49. Chauhan VP, Stylianopoulos T, Martin JD, Popović Z, Chen O, Kamoun WS, et al. Normalization of tumour blood vessels improves the delivery of nanomedicines in a size-dependent manner. Nat Nanotechnol. 2012;7(6):383–8.

50. Johnstone CN, Smith YE, Cao Y, Burrows AD, Cross RSN, Ling X, et al. Functional and molecular characterisation of EO771.LMB tumours, a new C57BL/6-mouse-derived model of spontaneously metastatic mammary cancer. Dis Model Mech. 2015;8(3):237–51.

51. Winkler F, Kozin SV, Tong RT, Chae S-S, Booth MF, Garkavtsev I, et al. Kinetics of vascular normalization by VEGFR2 blockade governs brain tumor response to radiation. Cancer Cell. 2004;6(6):553–63.

52. Miller DW, Vosseler S, Mirancea N, Hicklin DJ, Bohlen P, Völcker HE, et al. Rapid vessel regression, protease inhibition, and stromal normalization upon short-term vascular

endothelial growth factor receptor 2 inhibition in skin carcinoma heterotransplants. Am J Pathol. 2005;167(5):1389–403.

53. Alam A, Blanc I, Gueguen-Dorbes G, Duclos O, Bonnin J, Barron P, et al. SAR131675, a potent and selective VEGFR-3–TK inhibitor with antilymphangiogenic, antitumoral, and antimetastatic activities. Mol Cancer Ther. 2012;11(8):1637–49.

54. Espagnolle N, Barron P, Mandron M, Blanc I, Bonnin J, Agnel M, et al. Specific inhibition of the VEGFR-3 tyrosine kinase by SAR131675 reduces peripheral and tumor associated immunosuppressive myeloid cells. Cancers (Basel). 2014;6(1):472–90.

55. Shigeta K, Datta M, Hato T, Kitahara S, Chen IX, Matsui A, et al. Dual programmed death receptor-1 and vascular endothelial growth factor receptor-2 blockade promotes vascular normalization and enhances antitumor immune responses in hepatocellular carcinoma. Hepatology. 2020;71(4):1247–61.

56. Kerbel RS, Yu J, Tran J, Man S, Viloria-Petit A, Klement G, et al. Cancer Metastasis Rev. 2001;20(1/2):79–86.

57. Fukino, K. *et al.* (2003) 'Genetic background influences therapeutic effectiveness of VEGF', *Biochemical and Biophysical Research Communications*, 310(1), pp. 143–147. doi: 10.1016/j.bbrc.2003.08.134.

58. Nakao, S. *et al.* (2010) 'Lymphangiogenesis and angiogenesis: concurrence and/or dependence? Studies in inbred mouse strains', *The FASEB Journal*, 24(2), pp. 504–513. doi: 10.1096/fj.09- 134056.

59. Cunha F, Martins L, Martin PK, Stilhano R, Han S. A comparison of the reparative and angiogenic properties of mesenchymal stem cells derived from the bone marrow of BALB/c and C57/BL6 mice in a model of limb ischemia. Stem Cell Res Ther. 2013;4(4):86.

60. Torok S, Rezeli M, Kelemen O, Vegvari A, Watanabe K, Sugihara Y, et al. Limited tumor tissue drug penetration contributes to primary resistance against angiogenesis inhibitors. Theranostics. 2017;7(2):400–12.

61. Marques, S. M. *et al.* (2011) 'Genetic background determines mouse strain differences in inflammatory angiogenesis', *Microvascular Research*. Elsevier Inc., 82(3), pp. 246–252. doi: 10.1016/j.mvr.2011.08.011.

62. Gavard, J. and Gutkind, J. S. (2006) 'VEGF Controls endothelial-cell permeability promoting β- arrestin-dependent Endocytosis VE-cadherin', *Nature Cell Biology*, 8(11), pp. 1223–1234. doi: 18910.1038/ncb1486.

63. Heinolainen, K. *et al.* (2017) 'VEGFR3 Modulates Vascular Permeability by Controlling VEGF/VEGFR2 Signaling', *Circulation Research*, 120(9), pp. 1414–1425. doi: 10.1161/CIRCRESAHA.116.310477.

64. Hamrah P, Chen L, Zhang Q, Dana MR. Novel expression of vascular endothelial growth factor receptor (VEGFR)-3 and VEGF-C on corneal dendritic cells. Am J Pathol. 2003;163(1):57–68.